euspen's 22nd International Conference & Exhibition, Geneva, CH, May/June 2022
www.euspen.eu

# Vision based diameter estimation for continuous float-zone silicon crystal growth production

Tingting Chen[1], Guido Tosello[1], Nico Werner[2], Matteo Calaon[1]

[1] *Technical University of Denmark, Produktionstorvet, 2800 Kgs. Lyngby, Denmark*
[2] *Topsil GlobalWafers, Siliciumvej 1, 3600 Frederikssund, Denmark*

*tchen@mek.dtu.dk*

**Abstract**
Diameter measurement of cylinder with vision system is of great importance for diameter control in the float-zone silicon crystal growth. Targeted for float-zone silicon crystal growth, a vision-based diameter measurement with estimated expanded uncertainty for large diameter scope, is presented. The method is developed over two steps: camera calibration, diameter measurement and correction. Firstly, camera calibration identifies intrinsic and extrinsic properties of camera. Intrinsic parameters of camera model are obtained from the pattern of a checkerboard in advance. Then extrinsic parameters are inferred by tracking corner points of checkboard while rotating the checkerboard around cylinder axis. Finally, with estimated intrinsic and extrinsic parameters, pseudo diameter can be determined from the image points and corrected into actual diameter by trigonometric principle.The effectiveness of the proposed method was experimentally verified by measuring cylindrical gauges with diameter ranging from 5 mm to 150 mm.

Diameter measurement; Vision system; Measurement uncertainty; Float-zone crystal growth

## 1. Introduction

With growth of wafer application in microelectronic and photovoltaic industries, the demand for wafer is rising as well. Silicon wafer manufacturing begins with crystal growth process where the polycrystalline silicon is crystalized into pure monocrystalline silicon. There are mainly two methods for silicon crystal growth process: Czochralski (CZ) method and Float-zone (FZ) method. Currently CZ Si wafers make up the vast majority of total Si wafer market [1] due to fast growth speed and large growth diameter. Nevertheless, the FZ method can offer unique properties of superior purity and high resistivity which the CZ method cannot achieve [2,3], and therefore the FZ silicon is indispensable for high power electronics and innovative devices [3]. In the FZ process, polycrystalline silicon (feed rod) is melted by contactless heater like radio frequency (RF) coil and grows into monocrystalline silicon with the help of contacted seed crystal [4]. The FZ process is normally controlled by automatic growth controller.

In the FZ process, diameter control plays an important role since it ensures the crystal grows in good shape and quality. On the other hand, keeping diameter into control can help reduce waste or scrap. Therefore, it is necessary to measure crystal diameter with high efficiency and accuracy for obtaining homogeneous crystal [5].

However, due to high temperature and vacuum atmosphere within the FZ machines, it is not possible to measure the growing crystal during process with contacting measuring equipment like caliper or micrometer. Therefore, optical measurement is preferred for FZ crystal diameter measurements. Normally, there is a quartz window in FZ machine for vision system to capture geometrical quantities of crystal, and diameter measurement problem turns into cylinder diameter measurement based on images.

Various methods on cylinder diameter measurements have been investigated during past decades and they can be mainly categorized into two methods: telecentric vision based measurements [6-8] and pinhole vison based measurements [9-11]. Due to constant magnification, telecentric vision can measure object with high accuracy regardless of object distance. However, the field of view (FOV) is limited in telecentric lens and the larger the required FOV, the larger diameter of front lens has to be. Considering FZ crystal diameter is up to 200 mm, the required telecentric lens will be very large and expensive.

Compared with telecentric lens, pinhole lens has higher FOV since there is an angle between light ray and optical axis by passing light ray through pinhole. However, when measuring a cylinder, since the light ray is tangent to the cylinder surface, the measured length is actually a 'pseudo diameter', the projection length of two tangent points. Hence, it is necessary to deal with the inconsistent diameter problem. Takesa et.al [12] measured cylinder diameter by measuring the 'pseudo diameter' with magnification factor and deriving actual diameter by trigonometric principle with focal length. However, in this method, the magnification factor was set constant after calibration while it varied with different diameters since tangent points vary. Wei and Tan [13] presented a diameter measurement method based on camera model parameters. Intrinsic parameters were calibrated with checkerboard and extrinsic parameters were determined by measuring reference shaft with non-linear optimization. With intrinsic and extrinsic parameters instead of magnification factor, the 'pseudo diameter' can be determined and corrected to actual diameter with trigonometric principle. Nevertheless, measuring accuracy is sensitive to initial estimate of extrinsic parameters due to the nature of non-linear optimization. Sun et.al [9] improved this by identifying intial extrinsic parameters from checkerboard which was clamped to embody the axis of shaft. Nonlinear optimization was then used for recalibrating extrinsic parameters. An average measurement error of 0.005 mm was finally achieved. Nonetheless, this was only tested on shafts with small diameters up to 30 mm. Moreover, in some cases it is difficult to utilize two center heads to clamp checkerboard in

order to reduce misalignment. Hao et.al [14] presented a new measuring scheme with a movable camera, which can derive diameter from two images at different object distances. However, though this method can achieve high accuracy, a single diameter measurement requires the camera to move two times, which would potentially increase measuring time and decrease the possibility of application in in-process measurement.

Motivated by Wei and Tan [13] and Sun et.al [9], this paper presented a pinhole-vision based diameter measurement method for float-zone silicon crystal growth production based on camera model parameters. Similarly, camera model parameters are calibrated first and then projection length computed from camera parameters is corrected into true diameter by trigonometric principle. There are two main contributions in this paper including:

1) A diameter measurement method targeted for large range cylinder diameter (5 mm to 200 mm) is presented and validated in both test bed and float-zone silicon crystal growth production.

2) Uncertainties for diameter measurement in this method are estimated for ensuring the traceability of the measurements.

## 2. Methodology

The proposed diameter measurement method involves two steps: (i) camera calibration and (ii) diameter measurement. Camera calibration computes camera properties as well as the relationship between the camera and the measuring plane, which is very significant because it directly determines measuring accuracy. With the obtained camera model parameters, the cylinder length in the image can be transformed into the pseudo diameter and then corrected with diameter correction model. The framework of the diameter measurement method is illustrated in Figure 1.

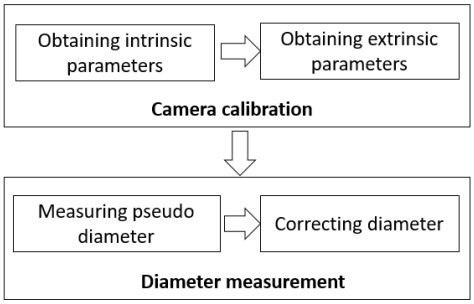


**Figure 1.** Framework of diameter measurement method

### *2.1. Camera calibration*

Camera calibration aims to compute intrinsic and extrinsic properties of camera pinhole model which is expressed in Eq 1.

$$s\begin{bmatrix} u \\ v \\ 1 \end{bmatrix} = \boldsymbol{K}[\boldsymbol{R}|\boldsymbol{t}]\begin{bmatrix} X \\ Y \\ Z \\ 1 \end{bmatrix} \quad (1)$$

where u and v are coordinates on pixel frame of image and and X, Y, Z are coordinates on world frame. $\boldsymbol{K}$ is intrinsic matrix and $\boldsymbol{R}$ and $\boldsymbol{t}$ are extrinsic rotation and translation respectively.

In this paper, intrinsic parameters are obtained by utilizing Zhang's method [15].

Extrinsic parameters determines the position and orientation relationship between camera and measuring plane. In order to measure diameter, measuring plane have to cover cylinder axis, as shown in Fig 2. Extrinsic parameters are normally obtained by solving camera model with corner points of checkerboard which is placed on measuring plane. However, it is not easy to let checkerboard cover the axis of shaft, unless using special fixture. In this paper, extrinsic parameters are computed by rotating checkerboard which can be seen in Fig 3.

The chekerboard is mounted onto the same shaft holder used to fix measured cylinder. As the checkerboard rotates, corner points on the checkerboard also rotate around the axis. The track of an individual corner point is supposed to be an arc or a circle with center point lying on the axis. Therefore by computing all center points from tracks of all corner points, an axis line can be obtained by fitting those center points.

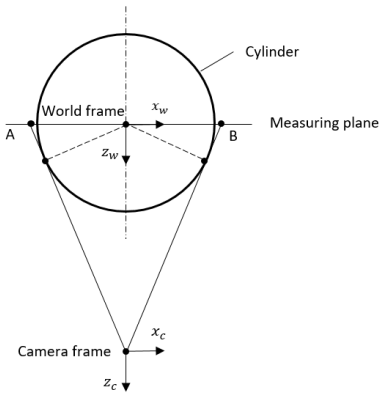


**Figure 2.** Relationship between camera frame and world frame

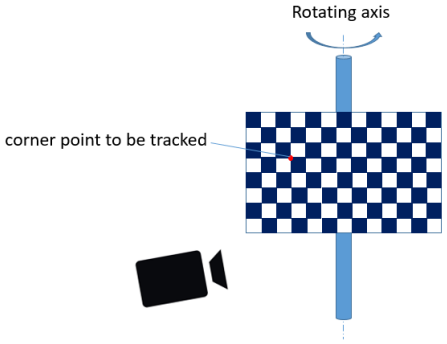


**Figure 3.** Rotating the checkerboard

Firstly, the camera frame is set as reference frame since it is static while world frame varies with rotation of checkerboard. Corner point $p_i$ $(i = 1,2,..,N)$ in checkerboard under world frame $\boldsymbol{W}_j$ $(j = 1,2,..,M)$ is expressed as $p_{wij}$, which can be computed by Eq 1 with estimated $\boldsymbol{R}_j$ and $\boldsymbol{t}_j$ from Zhang's method. Then $\boldsymbol{p}_{wij}$ is mapped into camera frame by the following equation.

$$p_{cij} = \boldsymbol{R}_j p_{wij} + \boldsymbol{t}_j \quad (2)$$

Where $p_{cij}$ is corner point $p_i$ in $j^{th}$ checkerboard image under camera frame.

Then extrinsic translation of our desired measuring plane $\boldsymbol{t}_m$ can be determined by averaging all points under camera frame, as Eq. 3 shows.

$$\boldsymbol{t}_m = \frac{1}{MN}\sum_{j=1}^{M}\sum_{i=1}^{N} p_{cij} \quad (3)$$

Apparently, all tracking circles' planes share the same normal vector $\boldsymbol{r}_y$, which is parallel to the axis of cylinder. $\boldsymbol{r}_y$ can be determined by minimizing the following objective function Eq 4.

$$min\sum_{j=1}^{M}\sum_{i=1}^{N}\left[(p_{cij} - o_{ci})\boldsymbol{r}_y^{\mathrm{T}}\right]^2 \quad (4)$$

Where $o_{ci}$ is the center point of tracked circle from corner point $p_i$, $o_{ci} = \frac{1}{M}\sum_{j=1}^{M} p_{cij}$.

Let $\boldsymbol{r}_x = (1,0,0)$ , $\boldsymbol{r}_z = \boldsymbol{r}_x \times \boldsymbol{r}_y$ , then desired extrinsic rotation $\boldsymbol{R}_m$ can be finally obtained.

$$\boldsymbol{R}_m = [\boldsymbol{r}_x, \boldsymbol{r}_y, \boldsymbol{r}_z] \quad (5)$$

### *2.2. Diameter measurement and correction*

With the obtained intrinsic parameters and extrinsic parameters from section 2.1, edge points of the cylinder in the image after undistortion can be transformed into world frame by Eq. 1. However, as above mentioned in section 1, the measured distance from a pair of edge points e.g. AB shown in Fig. 2, is actually pseudo diameter. Therefore it has to be corrected by using trigonometric principle.

It is assumed that the principal point of camera $O_c$ is slightly deviated from the center as shown in Fig 4, which is normally unavoidable situation.

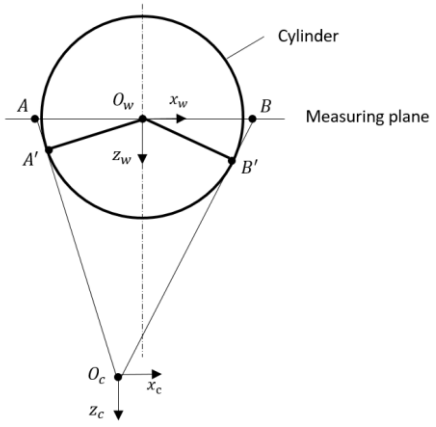


**Figure 4.** Deviated optical point

The principle point $O_c$ under the world frame is expressed as $O_{cw}$, which can be computed from extrinsic parameters $R_m$ and $t_m$, as shown in Eq. 6.

$$\boldsymbol{R}_m O_{cw} + \boldsymbol{t}_m = O_c = \begin{bmatrix} 0 \\ 0 \\ 0 \end{bmatrix} \tag{6}$$

Then the actual diameter can be computed with Eq 7.

$$\mathrm{D} = 2O_wA' = 2O_wO_{cw}sin\frac{\angle AO_{cw}B}{2} \tag{7}$$

here $\angle AO_{cw}B$ can be calculated based on the length AB, $\mathrm{A}O_{cw}$ and $\mathrm{B}O_{cw}$ with cosine theorem.

To improve measuring accuracy, the extrinsic parameters are recalibrated by measuring few cylindrical gauges with known diameter. The objective function for optimizing extrinsin parameters is shown as follows:

$$min\, S(\boldsymbol{R}, \boldsymbol{t}) \tag{8}$$

Where S = $\sum_{i=1}^{n}(D_{vi} - D_{ri})^2$. $D_{vi}$ is the reading from the proposed method and $D_{ri}$ is the reference diameter of the gauge.

## 3. Experiments

To verify the proposed method, the experiment work was performed by the camera with an image resolution of 1600 x 1200 pixels. To simulate the float-zone machine as shown in Fig. 6, the distance between the camera to the center of cylinder is around 1300 mm. The experimental setup is shown in Fig. 5. The image magnification factor is approximately 0.16 mm per pixel. The checkerboard with the corner points of 25x18 was used to calibrate the camera, in which the intrinsic matrix and distortion coefficients were inferred by Zhang's method [15]. Backlight was utilized in order to ensure the quality of image points and two coverings were used to reduce reflection from backlight [13]. The measurements were done in a temperature-controlled lab, set at (20 ± 0.2) °C.


**Figure 5.** Experiment setup

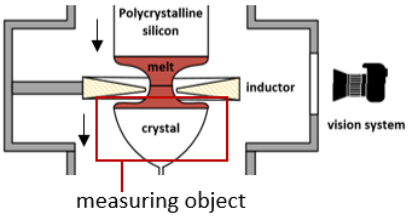


**Figure 6.** Float-zone crystal machine and vision system

For obtaining the extrinsic matrix in which the X-Y plane covers the rotating axis of the shaft, the checkerboard was rotated around the shaft axis while the camera captured images at the same time. Then extrinsic matrix was solved with the method presented in the section 2.1.

The step cylindrical gauge with diameter ranging from 5 mm to 150 mm, as shown in Fig 7, was used to test the accuracy of the proposed method. And extrinsic matrix was recalibrated by measuring gauges with diameter of 5 mm, 50 mm, 100 mm, 150 mm.

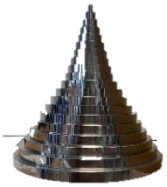

**Figure 7.** Step gauge

For comparison, the experiments were also conducted with the pixel-equivalent based method where the magnification factor instead was used to compute the pseudo diameter. The magnification factor in the pixel-quivalent method is calibrated and optimized with the least square method by cylindrical gauges with diameter of 5 mm, 10 mm, 15 mm, 20 mm since diameter correction can be neglected in small diameters. In the pixel-equivalent method, due to limited information, the corrected diameter can only be inferred from pseudo diameter and camera distance and assume the camera points at the axis of cylinder. The corrected diameter is computed by the following equation:

$$D_{vp} = \frac{CD_p}{\sqrt{C^2 + \left(\frac{D_p}{2}\right)^2}} \tag{9}$$

Where C is the camera distance and $D_p$ is the pseudo diameter obtained from image length and magnification factor.

We repeated capturing images of each cylindrical gauge for 30 times. For each repeated image, 34 pairs of feature points were used for diameter calculation and the average of diameters was considered to be the measured diameter.

Based on ISO 14253-2:2011 [16], results are provided with systematic error and an uncertainty analysis comprising the addition in uncertainty from reference gauge, resolution, and environment.

$$b_v = D_v - D_{ref} \tag{10}$$

Where $D_v$ is reading diameter from the proposed method, $D_{ref}$ is reference diameter from calibration certificate.

$$u_v = \sqrt{u_{ref}^2 + u_{res}^2} \tag{10}$$

Where $u_{ref}$ is the uncertainty contribution related to reference gauge, $u_{res}$ is the standard uncertainty contribution of resolution, Since feature points were detected by sub-pixel edge detection, we considered the resolution was 0.3*magnification factor*2 (since there is a pair of points involving diameter calculation). The expanded uncertainty $U_v$ is expressed as:

$$U_v = k \times u_v \quad (11)$$

Where k is the coverage factor(k=2 provides a confidence level of approximately 95% ).

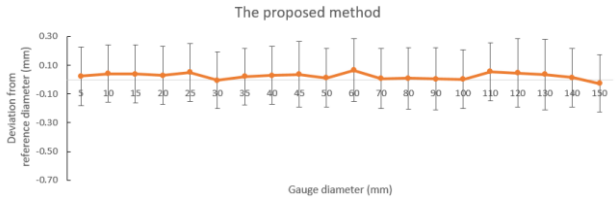


**Figure 8.** Measurement results using the proposed method

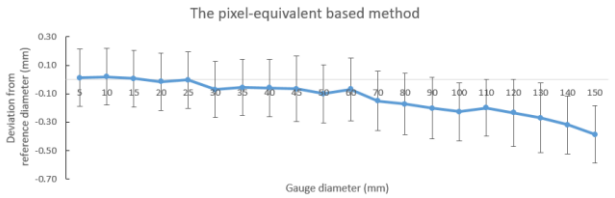


**Figure 9.** Measurement results using the pixel-equivalent method

From Fig. 8 and Fig. 9 we can notice a relatively large uncertainty of approximately $\pm 0.2$ mm, which is due to low resolution of image. However, in the proposed method, deviations from the reference diameter is almost invariant with gauge diameters, keeping the error into the range of $\pm 0.1$ mm.

On the contrary, in the pixel-equivalent method, a slightly increasing trend can be noticed. Two reasons may explain it. On one hand, lens distortion is not taken into account. As the gauge diameter increases, the edges are more far away from the image center, and distortion is therefore more serious. On the other hand, poor precision of magnification factor can also affect measuring accuracy. Since the magnification factor is inferred from the number of pixels in the image and the actual diameters, magnification factor is sensitive to the resolution of image which is relatively low in this experiment.

In summary, compared with the pixel-equivalent based method, the proposed method shows more robustness when measuring cylinders with large diameter scope. This proves the effectiveness of using normal fixture to infer extrinsic parameters, which may address the need of special fixture to compute accurate initial extrinsic parameters.

## 4. Conclusion

In this study, we proposed a diameter measurement method for cylinders ranging from 5 mm to 150 mm without using any special fixture, which is targeted for float-zone crystal growth production. The checkerboard was utilized to compute camera parameters. However, in extrinsic calibration, instead of placing the checkerboard where the cylinder axis is covered, we rotated checkerboard along the axis and inferred the position and orientation of cylinder axis from the recorded corner points of checkerboard. Experiments show that the measurement error can be kept into around $\pm 0.1$ mm.

In this study the measurement accuracy of a vision-based diameter and its measurement uncertainty in a longer diameter scope are investigated. Our results provide compelling evidence that diameter measurements utilizing camera parameters appear to be more robust than the pixel-equivalent method. This result can lay the foundation for diameter control in crystal growth of silicon where tracking diameters from few millimeters up to 200 mm is needed. Future work will focus on applying the method in crystal growth images.

However, some limitations are worth noting. Although the proposed method was supported statistically, the obtained accuracy was lower than previous results [9][13]. Though this is partially due to lower resolution and longer camera distance, both feature point detection and vibration of rotating axis also remarkably affect measurement accuracy. Future work should, therefore, include addressing the solution to evaluate the measurement uncertainty due to vibrating axis.


## Acknowledgements

This research work was undertaken in the context of DIGI-MAN4.0 project ("DIGItal MANufacturing Technologies for Zero-defect Industry 4.0 Production", http://www.digiman4-0.mek.dtu.dk/). DIGIMAN4.0 is a European Training Network supported by Horizon 2020, the EU Framework Programme for Research and Innovation (Project ID: 814225).


## References


[1] Zulehner, Werner. Historical overview of silicon crystal pulling development. *J. Materials Science and Engineering: B* **73**.1-3 (2000): 7-15.

[2] Müller, Georg, Jean-Jacques Métois, and Peter Rudolph, eds. *B. Crystal Growth-From fundamentals to technology*. Elsevier, 2004. **1** 239.

[3] Muiznieks, Andris & Virbulis, Janis & Lüdge, Anke & Riemann, Helge & Werner, Nico. *B. Floating Zone Growth of Silicon*, Elsevier, 2015. **7** 244

[4] Shimura, Fumio. Single-crystal silicon: growth and properties. *B. Springer Handbook of Electronic and Photonic Materials.* Springer, Cham, 2017. **1** 1.

[5] Wang, X., Xiang, S., Xiang, K., & Pan, F. (2018). A novel method for diameter measurement of silicon single crystal. *J. Measurement*, **121**, 286-293.

[6] Yang, Zhao, et al. Research on imaging system of vision measurement for the shaft *MIPPR 2015: Remote Sensing Image Processing, Geographic Information Systems, and Other Applications*. International Society for Optics and Photonics, 2015. **9815**

[7] Chen, Jun, et al. Vision-based online detection system of support bar. In: *2016 IEEE International Conference on Information and Automation (ICIA)*. IEEE, **2016**. 1594-1599.

[8] Shuxia, Guo, et al. Mini milling cutter measurement based on machine vision. *Procedia Engineering*, 2011, **15** 1807-1811.

[9] Sun, Qiucheng, et al. Shaft diameter measurement using a digital image. *Optics and Lasers in Engineering*, 2014, **55** 183-188.

[10] Rakhmanov, V. V., et al. Cylinder diameter measurement with displacement and rotation error correction for non-telecentric optics. *In: Journal of Physics: Conference Series*. IOP Publishing, 2020. **1675** 012085.

[11] Sun, Qiucheng, et al. A planar-dimensions machine vision measurement method based on lens distortion correction. *The scientific world journal*, 2013, **2013**.

[12] Takesa, Kazuhiko, et al. Measurement of diameter using charge coupled device (CCD). *CIRP annals*, 1984, **33** 1 377-381.

[13] Wei, Guang; Tan, Qingchang. Measurement of shaft diameters by machine vision. *Applied optics*, 2011, **50** 19: 3246-3253..

[14] Hao, F., et al. Shaft diameter measurement using digital image composition at two different object distances. *In: IOP Conference Series: Materials Science and Engineering*. IOP Publishing, 2019. **504** 012097.

[15] Zhang, Zhengyou. A flexible new technique for camera calibration. *IEEE Transactions on pattern analysis and machine* intelligence, 2000, **22** 11: 1330-1334.

[16] Gashi, Bekim V. Technical Committee: ISO/TC 213 Dimensional and geometrical product specifications and verification: ISO 14253-2: 2011; Geometrical product specifications (GPS)—Inspection by measurement of workpieces and measuring equipment—Part 2: Guidance for the estimation of uncertainty in GPS measurement, in calibration of measuring equipment and in product verification. 2011.